J Mol Model (2013) 19:2965–2969
DOI 10.1007/s00894-013-1823-y

ORIGINAL PAPER

Tunable differential conductance of single wall C/BN nanotube heterostructure

Huaping Xiao · Chuanxiao Zhang · Kaiwang Zhang · Lizhong Sun · Jianxin Zhong

Received: 17 November 2012 / Accepted: 10 March 2013 / Published online: 5 April 2013

Abstract The transport properties and differential conductance of the heterostructures constructed by (5,5) single wall carbon nanotube (SWCNT) and (5,5) single wall boron nitride nanotube (SWBNNT) are investigated using density functional theory in combination with non-equilibrium Green's functions. We find that the transmission conductance of (5,5) BN/C nanotube heterostructure is not only continually depressed as the BNNT region increases but also the drop of the conductance is uniform in the energy window (−1.43 eV, 1 eV), which leads to linear I–V dependence for the systems when the bias is within this energy range. Moreover, the differential conductance linearly decreases when $n \leq 3$ but exponentially decreases when $n \geq 3$ for $(5,5)(BN)_n$/C heterostructure. Such tunable differential conductance of (5,5) BN/C nanotube heterostructure mainly derives from the blockage of the transport channels induced by the semiconductive BN segment.

Keywords C/BN nanotube heterostructure · Differential conductance · Transport property

PACS 72.15.Rn · 73.63.Fg · 72.10.Fk

Introduction

Carbon nanotubes (CNTs) are important potential materials for future molecular and nano electronics, because of their excellent electronic and optical properties [1, 2]. So far, many prototypic devices based on CNTs have been realized, such as field-effect transistors, rectifiers, single-electron transistors, sensor and random access memory [3–8]. As its sister low dimensional system, boron nitride nanotubes (BNNTs) [9] also draw great attention due to their potential applications in nano-electronics and opto-electronics. Because their electronic properties depend much less on the specific nanotube geometry than their counterpart CNTs [10, 11], BNNTs are more amenable than CNTs to applications in electronics and opto-electronics. Subsequent to the discovery of CNTs and BNNTs, the hybrid systems of CNTs and BNNTs attract increasing interests due to their novel electronic properties and potential applications in nanotechnology. The hybrid nanotube provides us with not only a reliable and economical way to achieve nanotube herterojunctions for rectifying diodes, light emitting diodes and transistors but also an effective method to manipulate the electronic structures of nanotubes.

Using arc discharge [12, 13], laser ablation [14, 15], and chemical vapor deposition (CVD) [16], homogeneous BCN composition or phase separated BN and C layers have been successfully prepared. Moreover, using CVD method Liao et al. [17] directly synthesize massive BCN/C nanotube junctions and they found that the BCN/C nanotube junctions show a typical rectifying diode behavior hoping to achieve a variety of applications in electronic and optoelectronic device. Using ab initio calculations, Meunier et al. [18] showed that BN/C heterostructured nanotubes can be used for effective band-offset nanodevice engineering, polarization-based devices, and robust field emitters with an efficiency enhanced by up to two orders of magnitude over carbon nanotube systems. Using the average bond energy method, Liu et al. [19] found that the valence and conduction band offsets of the heterojunction formed by (8, 0) CNT and BNNT are 1.83 and 0.79 eV. Fan et al. [20] not only found the dependence of the band offsets of (9, 0) and (10, 0) BN/C heterostructured

H. Xiao · C. Zhang · K. Zhang · J. Zhong (✉)
Laboratory for Quantum Engineering and Micro-Nano Energy Technology, Xiangtan University, Xiangtan, Hunan 411105, People's Republic of China
e-mail: jxzhong@xtu.edu.cn

L. Sun (✉)
Department of Physics, Xiangtan University, Xiangtan, Hunan 411105, People's Republic of China
e-mail: lzsun@xtu.edu.cn

nanotubes on the charge redistribution but also predicted that such heterostructured nanotubes have remarkably enhanced field-emission properties. The tunable bandgap and stability are also shown in hybrid nanotubes rolling from GNRs and BNNRs by ab initio calculations [21, 22]. Blase et al. [23] found that the junctions between GNRs and BNNRs are energetically stable and their electronic characteristics are largely independent of the radius, helicity, multiplicity, or degree of perfection of the constituting nanotubes. Moreover, they predicted that a true metal/insulator junction could be used as a Schottky barrier. Khalfoun et al. [24] demonstrated that a BN pair exhibits a transparency behavior for conduction electron and that the localization phenomenon is recovered when B and N atoms are no longer adjacent. They also found that the conduction plateau has quasi-linear decrease as the BN domains increase. Fan et al. [25] reported that the interface states and steplike static potential profile appear in the band gaps of (5,5) BN/C nanotube heterostructures. Such interface states and potential profile will influence the transport properties. However, how the transport properties of (5,5) BN/C nanotube heterostructure depend on the size of the segment of BN is still an open question. To this end, we study the dependence of the transport properties and differential conductance of (5,5) BN/C nanotube heterostructure on the size of the BN segment using density functional theory in combination with non-equilibrium Green's functions. We find that the transmission conductance of (5,5) BN/C nanotube heterostructure is continually and uniformly depressed in the energy window (−1.43 eV, 1 eV) as the BNNT region increases. Moreover, the differential conductance linearly decreases when $n \leq 3$ but exponentially decreases when $n \geq 3$ for $(5,5)(BN)_n/C$ heterostructure.

Computational details

To obtain the optimized structure, the Vienna ab initio simulation package (VASP) [26, 27] is adopted, which is based on the density-functional theory (DFT) within the framework of projected augmented wave (PAW) [28, 29] and the Perdew-Burke-Ernzerhof (PBE) version of the generalized gradient approximation (GGA) [30]. A plane-wave basis set with the kinetic energy cutoff of 500 eV is employed. In geometry optimization, the atoms are fully relaxed until the residual force is less than 0.01 eV $Å^{-1}$ and the total energies are converged to 10^{-5} eV. The one-dimensional (1D) irreducible Brillouin zone is represented by Gamma centered Monkhorst-Pack special k-point mesh of 1×1×7. We consider the supercell that contains 9 unit cell (U.C.) along the axis of SWCNT (5,5) (containing 180 atoms for perfect nanotube). The BN dimer rings are gradually substituted carbon dimer ring in the center of the supercell. In our supercell, the minimum distance between two neighbor images is taken as more than 10 Å so that the interaction between the nearest tubes is negligible. We perform the quantum transport calculations by using the Atomistix ToolKit (ATK) package [31, 32], which is based on the real-space, nonequilibrium Green's function formalism and DFT. The double-plus ζ polarization numerical orbital basis set is chosen for all atoms. The exchange and correlation potential are also approximated by GGA with PBE functional [30]. The mesh cutoff is set to 150 Ry and the convergence of total energies is set to 10^{-5} Ry. Transport occurs in the z direction and periodic boundary conditions are assumed in the plane perpendicular to current, i.e., the system extends infinitely along the x and y directions. In present work, we focus on the intrinsic transport property of (5,5) BN/C nanotube heterostructure. Therefore, following previous theoretical works [33, 34] we use the "transparent" carbon nanotube electrodes to eliminate the influence of hetero-contact. In our model, left and right semi-infinite electrodes are the perfect SWCNT (5,5) with 2 U.C. (40 carbon atoms), and the central region consists of over 10 U.C. made up of the (5,5) BN/C nanotube heterostructure. Figure 1 represents the two-probe schematic diagrams of (5,5) BN/C nanotube heterostructure with three BN dimer rings. We have tested the compatibility of the combination of the two different methods. The transmission spectra of the heterostructures relaxed by either VASP or ATK show the same characteristics. Thus, we combine the efficient aspects of both methods, namely, using VASP to relax the structures and ATK to obtain their transport properties. All the computational parameters used in our present work are optimized.

Results and discussion

In the present work, we focus on the dependence of the transport properties of (5,5) BN/C nanotube heterostructure on the size of BN dimer rings. We construct the heterostructure by gradually substituting the BN dimer rings into SWCNT (5,5). The heterostructures are denoted as $(5,5)(BN)_n/C$, where n is the number of the BN dimer rings. The structure of $(5,5)(BN)_3/C$ is shown in Fig. 1. All optimized heterostructures have smooth interfaces due to the bond match between BNNTs and CNTs. To evaluate the

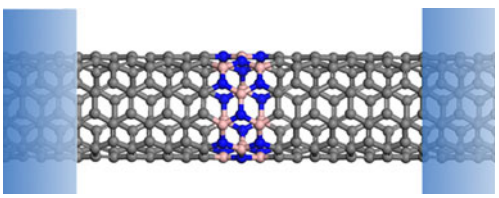

Fig. 1 Schematic description of the two probe system of (5,5) BN/C nanotube heterostructure with 3 BN dimer rings

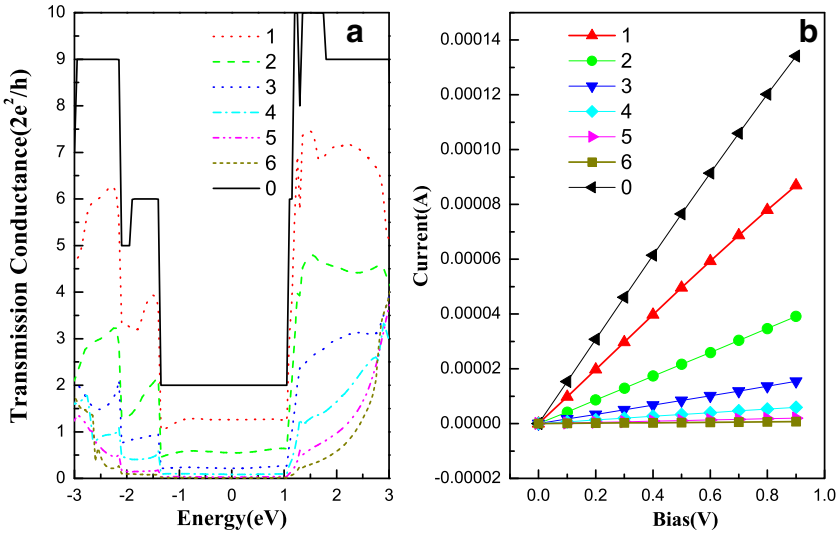

Fig. 2 Dependence of transmission spectra (**a**) and I–V curves (**b**) of (5,5)$(BN)_n$/C nanotube heterostructures on the size of BN dimer rings

stability of the heterostructures, the Gibbs free energy of formation δG is used, which is defined as [35]:

$$\delta G = E_{BN/C}(tot) - \chi_C \mu_C - \chi_{BN} \mu_{BN}, \quad (1)$$

where *E(tot)* is the cohesive energy per atom of the heterostructures with different compositions, χ_i is the molar fraction of atom i (i=*C*,*BN*) in the structure satisfying $\chi_C + \chi_{BN} = 1$, and μ_i is the chemical potential of each constituent atoms. We choose μ_C and μ_{BN} as the cohesive energies per atom of a SWCNT (5,5) and BNNT (5,5), respectively. Our calculated δG is 0.45~0.52 eV per bond of the interfaces. Because the Gibbs free energy of the formation δG is dependent on the molar fraction of the system, our results based on the supercell with 9 unit cell agree with previous predication [25].

Based on the optimized (5,5)$(BN)_n$/C nanotube heterostructures, we calculate the transmission spectrum of the heterostructures and the results are shown in Fig. 2(a). The transmission spectra of the pristine SWCNT (5,5) is also included here for comparison purpose. As for the pristine SWCNT (5,5), the transmission conductance has a platform with $2G_0$ within the energy window of (−1.4, 1.1) eV, which agrees well with previous studies. When the BN dimer rings are introduced into SWCNT (5,5)

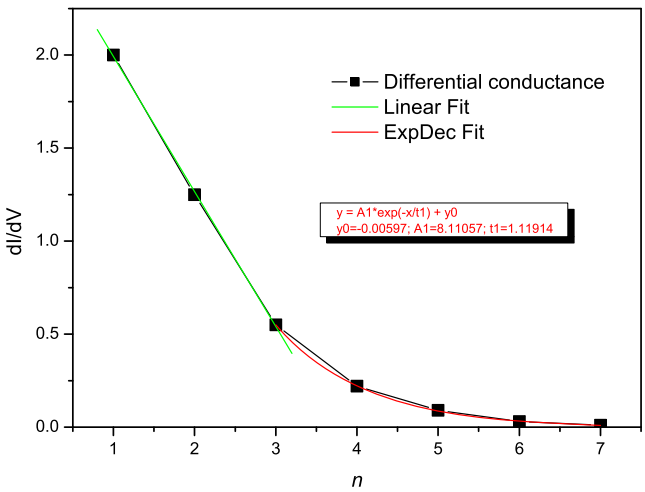

Fig. 3 Differential conductance of (5,5)$(BN)_n$/C in function of the size of the BN dimer rings

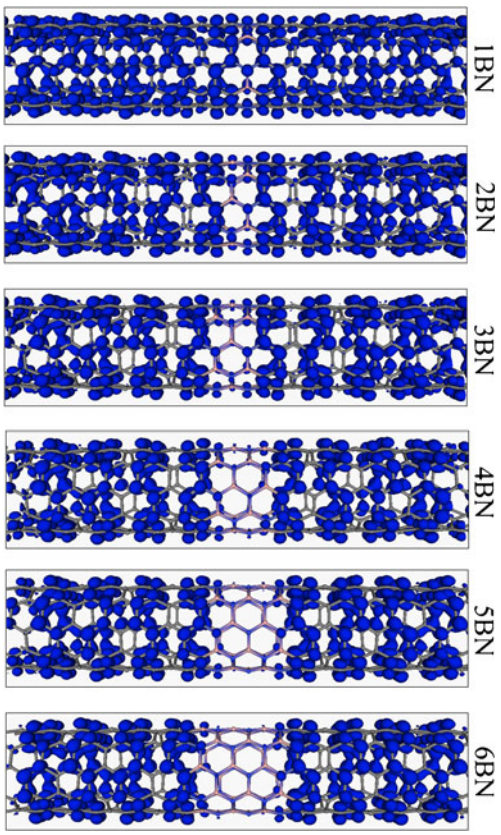

Fig. 4 Distribution of the LDOS at the Fermi level for (5,5)$(BN)_n$/C heterostructures

forming the heterostructure, the transmission conductance platform around the Fermi level is severely depressed. Interestingly, the energy window of the platform of the (5,5)$(BN)_n$/C heterostructures around the Fermi level remains as that of SWCNT (5,5). The transmission conductance at Fermi level of (5,5)$(BN)_n$/C is reduced from $2G_0$ to $1.25G_0$, $0.55G_0$, $0.22G_0$, $0.09G_0$, $0.03G_0$, and $0.01G_0$ as n increases from 0 to 6 with step 1. Such decrease is derived from the tunneling effect of the conduction electron of CNT through a wider and wider barrier forming by the semiconductive BN dimer rings. The reduction of the transmission conductance of the (5,5)$(BN)_1$/C nanotube heterostructures in comparison with that of pristine SWCNT (5,5) is similar to the results of BN codoped SWCNT (5,5) [24] when BN co-doping domain forms a complete ring. When the number of the BN dimer rings is larger than 6 a transmission gap of 2.5 eV appears.

To evaluate the transport properties of (5,5)nBN/C nanotube heterostructures in function of the BN dimer rings under un-equilibrium condition, we calculate the I–V curve of the systems as shown in Fig. 2(b). When the bias is within (0, 0.9)V, the I–V curves of all the systems show well linear characteristics. This indicates that the barrier of the heterostructures is very stable under the external bias. Such stability is derived from the platform of the transmission conductance around the Fermi level. Our results indicate that the (5,5)$(BN)_n$/C nanotube heterostructures can be potential tunable resistors for nanoelectronics. To quantitatively show such nature, we calculate the differential conductance of the heterostructures based on the I–V curves as shown in Fig. 3. The results indicate that the differential conductance of (5,5)$(BN)_n$/C nanotube heterostructures decreases linearly when the size of the BN ring is smaller than 4. While the size of the BN ring is larger than 2 the differential conductance exponentially decays as the the size of the BN segment increases. As indicated by Fan et al. [25], the CNT states decay rapidly within one atomic layer in BN segment of the interface of (5,5)$(BN)_n$/C nanotube heterostructures. The charge redistribution in the region near the interfaces set up build-in electric field, resulting in steplike static potential profiles in (5,5) BN/C nanotube heterostructures. When the size of the BN rings is less than 4, the barrier of the BN segment gradually increases with the increase of the size of the BN ring, resulting in the linear decay of the differential conductance. When the size of the BN ring is larger than 3, a complete barrier in the BN segment is formed and the barrier becomes wider with the increase of the BN ring. The transmission of the conduction electrons of CNT through such barrier follows the rule of tunneling effect through a quasi-square barrier, resulting in the exponential decay of the differential conductance.

In order to clearly show the depression mechanism of the differential conductance of (5,5)$(BN)_n$/C heterostructures with the increase in the BN segment, we calculated the local density of states (LDOS) at the Fermi level for all the heterostructures, as shown in Fig. 4. The LDOS qualitatively represents the distribution of transport channels at real space. We find that when $n \leq 3$ the LDOS quasi-continuously distributes along the nano heterostructures; and the LDOS around the BN segment decays gradually with the increase in the size of BN ring. Such distribution characteristics of the LDOS produce the differential conductance decreases linearly with the increase in the size of BN segment when $n \leq 3$. When the BN ring is larger than 3, the LDOS is totally separated by the BN segment. The electronic states around the Fermi level can not contribute to effective transport channels. The transmission of the conduction electrons originates from the tunneling. The possibility of transmission follows the rule of tunneling effect resulting in the exponential decay of the differential conductance with the increase in the size of the BN segment.

The discovery and large-scale synthesis of CNTs and BNNTs have attracted enormous attention due to their potential applications in future nanotechnology. Inspired by the comparability of atomic configuration between CNTs and BNNTs as well as the huge differences in their electronic properties, many nanotubes with different stoichiometries of B, N and C elements (BNCNTs) have been not only theoretically investigated but also successfully synthesized [12–16]. One of the most important merits of such hybrid BNCNTs for application in nanodevices is that their band structures can be modulated by changing their atomic composition and configuration. Althogh the nanotube heterostructures with sharp interface studied in our present work are hardly realized in the present experimental stage, the model and the results obtained from it are hoped to be a useful physical reference for further study of BNCNTs.

Conclusions

Using density functional theory in combination with non-equilibrium Green's functions, we find that the transport properties of (5,5)$(BN)_n$/C nanotube heterostructures can be continually and uniformly modulated by the the size of BN segment. Through modulating the size of the BN segment, the differential conductance of (5,5)$(BN)_n$/C nanotube heterostructures linearly decreases when $n \leq 3$ but exponentially decreases when $n \geq 3$. Such transport characteristics mainly derive from the blockage of the transport channels induced by the semiconductive BN segment.

Acknowledgments This work is supported in part by the Program for New Century Excellent Talents in University (Grant No. NCET-10-0169), the National Natural Science Foundation of China (No.10874143, 10774127), the Scientific Research Fund of Hunan Provincial Education Department (Grant No. 10K065).

References

1. Martel R, Schmidt T, Shea HR, Hertel T, Avouris P (1998) Single- and multi-wall carbon nanotube field-effect transistors. Appl Phys Lett 73:2447–2449
2. Son Y-W, Cohen ML, Louie SG (2007) Electric field effects on spin transport in defective metallic carbon nanotubes. Nano Lett 7:3518–3522
3. Liu C, Fan YY, Liu M, Cong HT, Cheng HM, Dresselhaus MS (1999) Hydrogen storage in single-walled carbon nanotubes at room temperature. Science 286:1127–1129
4. Yao Z, Postma HWC, Balents L, Dekker C (1999) Carbon nanotube intramolecular junctions. Nature 402:273–276
5. Bockrath M, Cobden DH, McEuen PL, Chopra NG, Zettl A, Thess A, Smalley RE (1997) Single-electron transport in ropes of carbon nanotubes. Science 275:1922–1925
6. Tans SJ, Devoret MH, Dai H, Thess A, Smalley RE, Geerligs LJ, Dekker C (1997) Individual single-wall carbon nanotubes as quantum wires. Nature (London) 386:474–477
7. Dumitrica T, Belytschko T, Yakobson BI (2003) Bond-breaking bifurcation states in carbon nanotube fracture. J Chem Phys 118:9485–9488
8. Rueckes T, Kim K, Joslevich E, Tseng G, Cheung C, Lieber CM (2000) Carbon nanotube-based nonvolatile random access memory for molecular computing. Science 289:94–97
9. Chopra NG, Luyken RJ, Cherrey K, Crespi VH, Cohen ML, Louie SG, Zettl A (1995) Boron nitride nanotubes. Science 269:966–967
10. Rubio A, Corkill JL, Cohen ML (1994) Theory of graphitic boron nitride nanotubes. Phys Rev B 49:5081–5084
11. Blase X, Rubio A, Louie SG, Cohen ML (1994) Stability and band gap constancy of boron nitride nanotubes. Europhys Lett 28:335–340
12. Weng-Sieh Z, Cherrey K, Chopra NG, Blase X, Miyamoto Y, Rubio A, Cohn ML, Louie SG, Zettl A, Gronsky AR (1995) Synthesis of B-*xC*-*yN*-*z* nanotubules. Phys Rev B 51:11229–11232
13. Suenaga K, Colliex C, Demoncy N, Loiseau A, Pascard H, Willaime F (1997) Synthesis of nanoparticles and nanotubes with well-separated layers of boron nitride and carbon. Science 278:653–655
14. Terrones M, Grobert N, Terrones N (2002) Synthetic routes to nanoscale B-*xC*-*yN*-*z* architectures. Carbon 40:1665–1684
15. Zhang Y, Gu H, Suenaga K, Iijima S (1997) Heterogeneous growth of B-C-N nanotubes by laser ablation. Chem Phys Lett 279:264–269
16. Bai XD, Guo JD, Yu J, Wang EG, Yuan J, Zhou WZ (2000) Synthesis and field-emission behavior of highly oriented boron carbonitride nanofibers. Appl Phys Lett 76:2624–2626
17. Liao L, Liu KH, Wang WL, Bai XD, Wang EG, Liu YL, Li JC, Liu C (2007) Multiwall boron carbonitride/carbon nanotube junction and its rectification behavior. J Am Chem Soc 129:9562–9563
18. Meunier V, Roland C, Bernholc J, Nardelli MB (2002) Electronic and field emission properties of boron nitride/carbon nanotube superlattices. Appl Phys Lett 81:46–48
19. Liu HX, Zhang HM, Song JX, Zhang ZY (2010) Electronic structures of an (8, 0) boron nitride/carbon nanotube heterojunction. J Semicond 31:013001–013003
20. Fan YC, Hou KY, Wang ZH, He T, Zhang XJ, Zhang HY, Dong JM, Liu XD, Zhao MW (2011) Theoretical insights into the built-in electric field and band offsets of BN/C Heterostructured zigzag nanotubes. J Phys D: Appl Phys 44:095405 (1–6)
21. Du AJ, Chen Y, Zhu ZH, Lu GQ, Smith SC (2009) C-BN single-walled nanotubes from hybrid connection of BN/C nanoribbons: prediction by ab initio density functional calculations. J Am Chem Soc 131:1682–1683
22. Zhang ZY, Zhang ZH, Guo WL (2009) Stability and electronic properties of a novel C-BN heteronanotube from first-principles calculations. J Phys Chem C 113:13108–13114
23. Blase X, Charlier J-C, De Vita A, Car R (1997) Theory of composite B-*xC*-*yN*-*z* nanotube heterojunctions. Appl Phys Lett 70:197–199
24. Khalfoun H, Hermet P, Henrard L (2010) B and N codoping effect on electronic transport in carbon nanotubes. Phys Rev B 81:193411 (1–4)
25. Fan YC, Zhao MW, He T, Wang ZH, Zhang XJ, Xi ZX, Zhang HY, Hou KY, Liu XD, Xia YY (2010) Electronic properties of BN/C nanotube heterostructures. J Appl Phys 107:094304 (1–6)
26. Grujicic M, Cao G, Singh R (2003) The effect of topological defects and oxygen adsorption on the electronic transport properties of single-walled carbon-nanotubes. Appl Surf Sci 211:166–183
27. Jhi S-H, Louie SG, Cohen ML (2000) Electronic properties of oxidized carbon nanotubes. Phys Rev Lett 85:1710 (1–4)
28. Blöchl PE (1994) Projector augmented-wave method. Phys Rev B 50:17953–17979
29. Kresse G, Joubert D (1999) From ultrasoft pseudopotentials to the projector augmented-wave method. Phys Rev B 59:1758–1775
30. Perdew JP, Burke K, Ernzerhof M (1996) Generalized gradient approximation made simple. Phys Rev Lett 77:3865 (1–4)
31. Brandbyge M, Mozos J-L, Ordejn P, Taylor J, Stokbro K (2002) Density-functional method for nonequilibrium electron transport. Phys Rev B 65:165401 (1–17)
32. Soler JM, Artacho E, Gale JD, Garcła A, Junquera J, Ordejn P, Snchez-Portal D (2002) The SIESTA method for ab initio order-N materials simulation. J Phys Condens Matter 14:2745–2779
33. Yan Q, Wu J, Zhou G, Duan W, Gu B-L (2005) Ab initio study of transport properties of multiwalled carbon nanotubes. Phys Rev B 72:155425 (1–5)
34. Garcła-Surez VM, Ferrer J, Lambert CJ (2006) Tuning the electrical conductivity of nanotube-encapsulated metallocene wires. Phys Rev Lett 96:106804 (1–4)
35. Hod O, Barone V, Peralta JE, Scuseria GE (2007) Enhanced half-metallicity in edge-oxidized zigzag graphene nanoribbons. Nano Lett 7:2295–2299